FLUCOME 2009
10th International Conference on Fluid Control, Measurements, and Visualization
August 17–21, 2009, Moscow, Russia

COLLISION DYNAMICS OF RED BLOOD CELLS USING HIGH-SPEED IMPINGING MICROJETS

Takanobu Yagi[1], Shotaro Wakasa[1], Natsuko Tokunaga[1], Yuki Akimoto[1] and Mitsuo Umezu[1]

ABSTRACT

Elucidating the mechanism of flow-induced blood damage, such as hemolysis, plays an important role for arterial diseases and artificial organs. This study for the first time demonstrates the visualization of hemolysis in a single-cell real-time fashion using high-speed microfluidic technology. Impinging microjets with a velocity of 1.5 m/s order at a nozzle exit are made in the Y- and T-shaped microchannel, where the curved (r=10μm) and flat collision surface are compared respectively. Porcine fresh erythrocytes are suspended in phosphate buffered saline at the volume fraction of 0.5%. Results show that membrane failure is only observed in the Y-junction. These erythrocytes are initially elongated at the far region, and then longitudinally compressed in the near wall region. The counterparts in the T-junction, however, do not show such a longitudinal deformation at the same flow rate. With an aid of the numerical simulation of energy balance, it is found that the dominant force for the longitudinal compression is the pressure difference per erythrocyte. Erythrocytes in the Y-junction show the sudden drop of elastic modulus, suggesting that the elongated spectrin network of erythrocyte is fragile for the compressive force and immediately broken by the impact force.

Keywords: Micro, Jet, Red blood cell, Hemolysis

INTRODUCTION

Flow-induced blood cell damage, such as hemolysis, promotes thrombus formation in circulating blood. Over the last half century, enormous amount of studies have been carried out for better understanding of the underlying mechanism. At present, shear stress may be widely believed to play a dominant role for the damage. This knowledge derives from a long-term history of in vitro experiments using flow devices, such as rotational viscometers (for example, see Paul et al., 2003). After forcing cells to be exposed by the *steady* shear stress during a certain period of time, the damage is quantified by measuring the hemoglobin in plasma in an end-point fashion. In this idealized condition, however, the physical mechanism of hemolysis is still in hypothesis (Zhao et al., 2006; Watanabe et al., 2006).

We previously studied the flow dynamics of prosthetic valves, which has widely considered to induce blood damage. A novel analysis using time-resolved particle image velocimetry and continuous wavelet transform enabled modeling of the dynamics of anomalous flows, such as turbulence and closing flow, for circulating cells, resulting in the hypothesis that these abnormal flows promote the collision of flowing cells (Yagi et al., 2006). In other words, we hypothesize that flow-induced hemolysis in actual environments may not be dominated by the steady shear stress, but also by impulsive force upon collision, or dynamical complex loading, as encountered in actual flows.

[1] Corresponding author: T. Yagi, Integrative Bioscience and Biomedical Engineering, TWIns, Waseda University, Japan
e-mail: takanobu_yagi@akane.waseda.jp

In this study, we aim to verify the above hypothesis using microfluidic technology that can emulate the high traveling speed (m/s order) of blood cells in arterial flows. We have for the first time succeeded in visualizing single-cell and real-time hemolysis. This study not only addresses such visualizations, but also the dynamical mechanics of impact fracture of erythrocyte membrane upon collision.

EXPERIMENTAL METHODS

Fresh porcine venous blood was centrifuged at 1000 g for 5 min. After removing the plasma and buffy coat, erythrocytes were washed three times in phosphate buffer saline (PBS). Erythrocytes were suspended at a hematocrit of 0.5 % in PBS with porcine serum albumin (Sigma Aldrich, U.S.A.) at a concentration of 5.5×10^{-2} g/dl. The flow was made in a PDMS-made microchip as driven by a syringe pump at a constant flow rate. Temperature was adjusted at 37°C. Imaging was carried out using a high-speed camera (Fastcam 1024, Photron Limited, Japan) equipped with a zooming microscope (DZ3, Union Optical Co., Ltd., Japan) (Fig.1). Two channel geometries, or Y/T-junction, were compared with the same flow rate (Fig.2). The former had a curved collision surface (r=10 μm), and the latter had a flat surface. Both channels included a micro nozzle and diffuser at the upstream and downstream of the collision surface.

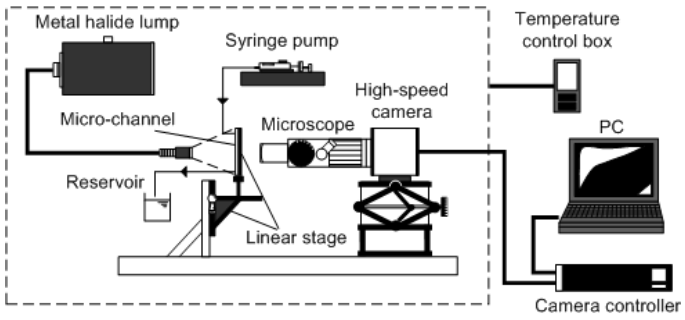

Fig.1 Schema of experimental setup

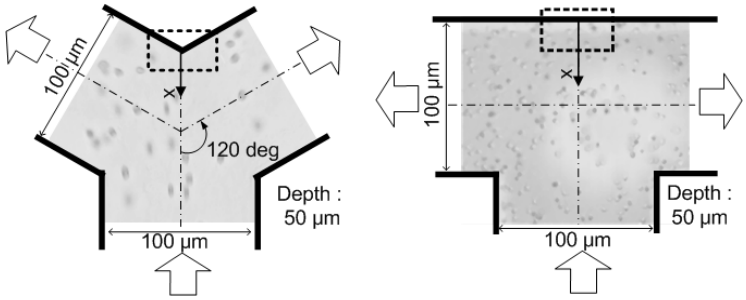

Fig.2 Geometry of channels

RESULTS

We firstly compared the traveling velocity and geometry of erythrocytes between channels as a function of distance from a collision surface (Fig.3). At X=80μm, erythrocytes showed the similar velocity (U_r~1.5m/s) and elongation (L/W~2.6) between channels, where L and W denote length and width of cells in a flowing direction, respectively. Near the collision surface, the slope of traveling velocity was about 2.3 times greater in the Y-junction. While these erythrocytes maintained the elongated shape (L/W~2.0) just before collision, those in the T-junction changed the shape dramatically (L/W~0.7).

Furthermore, while the width of erythrocytes in the T-junction started to increase from X=40μm, the counterpart in the Y-junction was even constant just before collision. In other words, erythrocytes in the Y- and T-junction were longitudinally and laterally compressed, respectively.

The impact fracture of erythrocytes was only observed in the longitudinal compression (Fig.4). Those erythrocytes underwent buckling upon collision, and their membrane collapsed immediately (white arrow). Then, intracellular substances were ejected out of the membrane. Note that these transient phenomena occurred in a microsecond order. Fig.5 shows characterization of erythrocyte geometries upon collision with respect to varying flow rates, which was standardized as an averaged fluid velocity U_n at the nozzle exit. In the Y-junction, erythrocytes upon collision were even elongated at a lower flow rate, whereas those in the T-junction showed the transience from the lateral to longitudinal compression as the flow rates increased. Taken together, it was suggested that the compression type of erythrocytes was closely related with the deceleration rate near the collision surface.

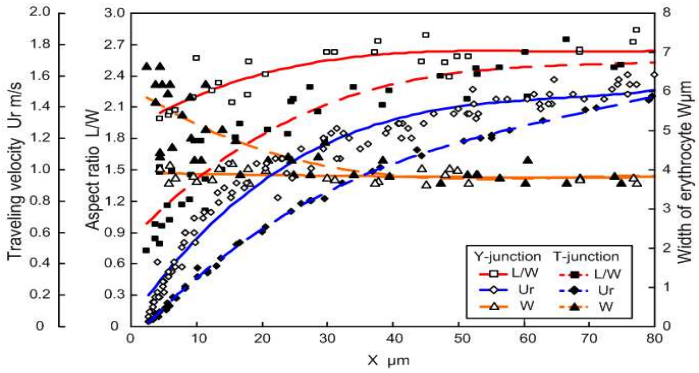

Fig.3 Traveling velocity and geometry of erythrocyte as a function of distance

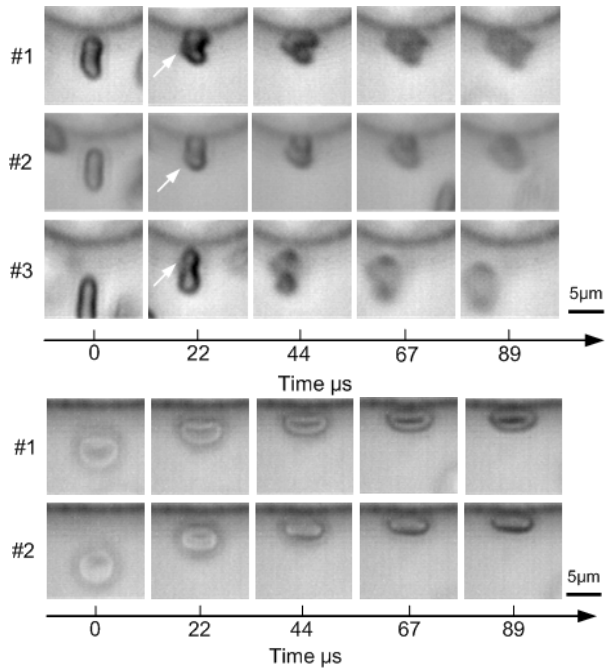

Fig.4 High-speed imaging of impact fracture of erythrocyte membrane upon collision (Top: Y-junction, Bottom: T-junction)

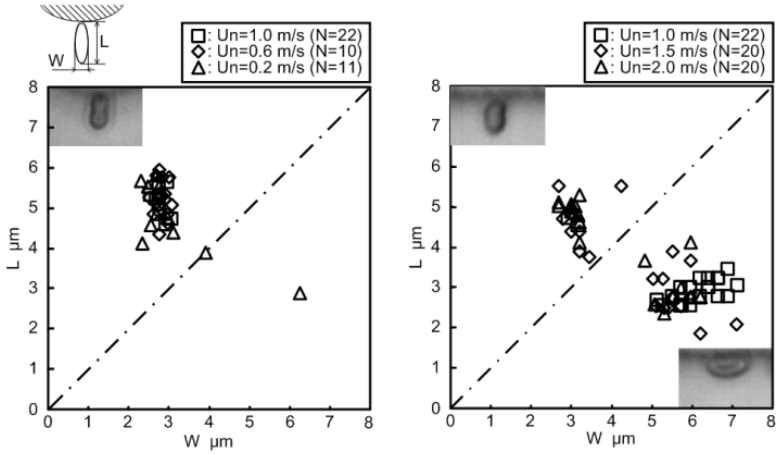

Fig.5 Geometry of erythrocytes upon collision for varying flow rates
(left: Y-junction, right: T-junction)

DISCUSSION

It would be essential to understand the dominant force for the longitudinal compression using a simplified one-dimensional model. Fig.6 shows the assumption of fluid forces on erythrocyte during a sharp deceleration. Determination of fluid velocity U_F in the vicinity of membrane would be beyond the scope of this study. Herein, U_F-U_R was assumed to be negligible, namely no relative motion. A single-phase numerical simulation was carried out by commercial software (Fluent 6.3.26, ANSYS, Inc.). In brief, the flow was simulated with the same flow rate (18.0 mL/h) by assuming Newtonian fluid (water at 20°C) with no slip on boundaries. The total number of mesh was around 1×10^6.

Fig.7 shows simulated results. In Fig.8, static pressure was plotted with the pressure difference for a single erythrocyte, or $dP_r=P_u-P_d$, which was obtained as follows,

$$dP_r(x)=\frac{dP}{dx}L(x) \tag{1}$$

where dP/dx was the pressure gradient (simulated value) and L(x) was the length of erythrocyte (experimental value). As seen in Fig.8, the pressure difference for a single cell in the Y-junction increases linearly and reaches a few hundreds of Pa just before collision, whereas the counterpart in the T-junction peaked at X=55μm, and decreased to be zero near the collision surface, namely erythrocytes being released out of the compressive force.

Then, energy balance for a single erythrocyte was analyzed to determine whether the pressure difference plays a dominant role for the longitudinal compression. Erythrocytes altered their geometry and traveling velocity owing to the adverse pressure gradient. The following relationship,

$$\Delta W\left(dP_r(x),A(x)\right)=\Delta K\left(U_r(x)\right)+\Delta E\left(L(x),k(x)\right) \tag{2}$$

exists, where ⊿W, ⊿K, and ⊿E denote the change of external work, kinetic energy, and strain energy,

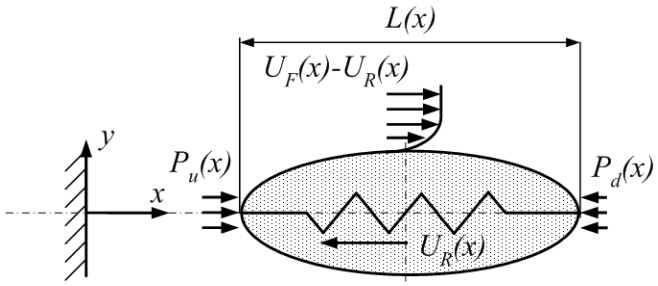

Fig.6 Schema of one-dimensional spring model of erythrocyte during deceleration

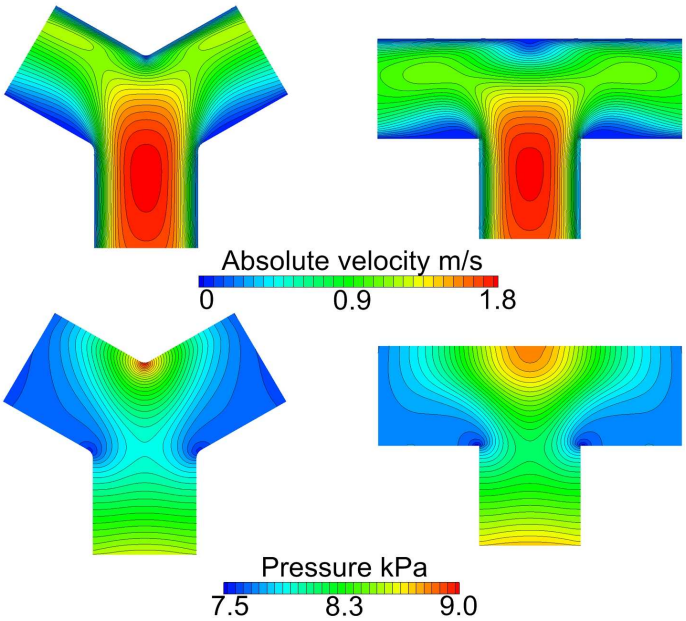

Fig.7 Results of numerical simulation (top: velocity, bottom: pressure).
Data was represented at a mid-depth plane.

respectively. The value A and k indicate the area and elastic modulus of erythrocyte. Note that the rotational motion of erythrocytes was assumed to be negligible. The external work and kinetic energy was obtained using the followings,

$$\Delta W\left(dP_r(x), A(x)\right) = \int dP_r(x)A(x)dx \tag{3}$$

$$\Delta K\left(U_r(x)\right) = \int m\frac{dU_r}{dt}dx \tag{4}$$

where A(x) was estimated by $A=\pi W^2/4$, and the mass of a single erythrocyte was assumed to be 9.8×10^{-14} kg. We assumed erythrocytes were initially located at x=80μm, and then calculations were carried out step-by-step in order to obtain the varying rate of external work and kinetic energy as a function of distance. By using equations (2-4), we can obtain the varying rate of strain energy, which is then used to

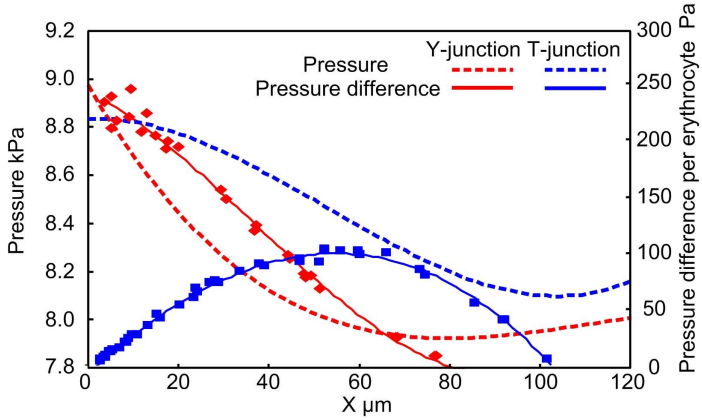

Fig.8 Plot of pressure and estimated pressure difference per erythrocyte

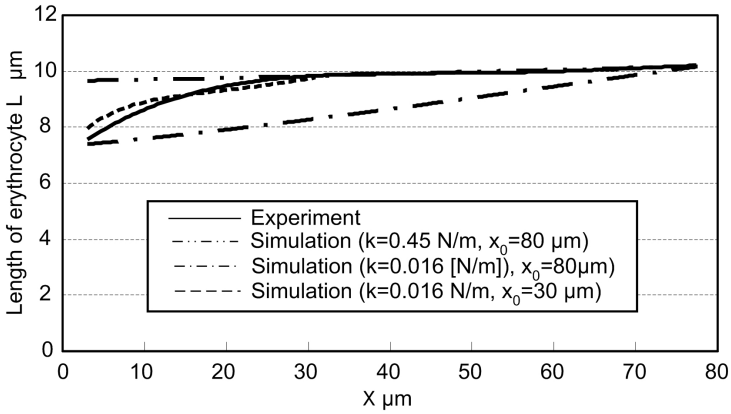

Fig.9 Length of erythrocyte as a function of distance.
x_0 denotes the initial location for calculating energy balance.

estimate the length of erythrocyte using the following relationship.

$$\Delta E(L(x),k(x)) = \frac{1}{2}k(x)(L(x+dx)-L(x))^2 \tag{5}$$

The initial location was set at x=80μm, where the length of erythrocyte was 10.2μm. The two elastic moduli, k=0.45 and 0.016N/m, were compared. The former was the area compressibility modulus for the red cell membrane (Waugh & Evans, 1979). The latter corresponded to that just before hemolysis, which was obtained by assuming a 5nm-thick membrane (Fung, 1993; Skalak et al., 1973). The results were plotted in Fig.9. Up to x=30μm, the simulated value using k=0.45 N/m was in good agreement with experiments, whereas the counterpart at k=0.016 N/m immediately deviated. In the near-wall region, however, the elastic modulus of k=0.45 N/m showed a large bias as erythrocytes being compressed. Then, we recalculated the length from x=30μm assuming k=0.016N/m, and then results agreed well with experiments.

From the above analysis, some interpretations can be derived. First of all, the membrane elasticity was sharply reduced by about 96% in the near-wall region as erythrocytes underwent the longitudinal compression. This implied that the spectrin no longer worked as an elastic platform of red cell membrane. It was speculated that the spectrin network was locally protruded by receiving the impact compressive force. Furthermore, the dominant force for the longitudinal compression was found to be the pressure difference per erythrocyte. The effect of shear stress was negligible as assumed as far as the compressive deformation is concerned. However, it may have a secondary effect as a binding force for the lateral deformation of erythrocyte.

CONCLUSION

To the best of our knowledge, we for the first time succeeded in visualizing single-cell real-time hemolysis in dynamical flow conditions. Colliding erythrocytes were characterized by the longitudinal and lateral compressive deformation depending on the deceleration of traveling erythrocytes. A dominant force for the longitudinal compression was the pressure difference per erythrocyte. These erythrocytes immediately lost their elasticity, indicating that the elongated spectrin network was fragile to the compressive loading, readily causing buckling and impact fracture. Present results indicate the importance of the dynamics of blood flow for hemolysis. In this study, we have successfully achieved to verify our hypothesis based on modeling of prosthetic valve flow.

ACKNOWLEDGMENTS

This research was partly supported by Health Science Research Grant (H20-IKOU-IPAN-001) from Ministry of Health, Labour and Welfare, Japan and the Grant-in-Aid for Scientific Research (21700474) from Ministry of Education, Culture, Sports, Science and Technology, Japan.

REFERENCES

Paul R, Apel J, Klaus S, Schugner F, Schwindke P, Reul H (2003), “Shear stress related blood damage in laminar couette flow,” Artificial Organs, 27(6), 517-529.

Zhao R, Antaki JF, Naik T et al. (2006), “Microscopic investigation of erythrocyte deformation dynamics,” Biorheology, 43, 747-765.

Watanabe N, Kataoka H, Yasuda T and Takatani S (2006), “Dynamic deformation and recovery response of red blood cells to a cyclically reversing shear flow: effects of frequency of cyclically reversing shear flow and shear stress level,”, Biophysical Journal, 91, 1984-1998.

Yagi, T., Akutsu, T., and Umezu, M. et al. (2006), “Real-time planar spectral analysis of instantaneous high-frequency stress on blood cells downstream of an artificial heart valve,” Proceedings of the 12th International Symposium on Flow Visualization.

Waugh R and Evans E.A. (1979), “Thermoelasticity of red blood cell membrane,” Biophys. J. 26, 115-132.

Fung Y.C. (1993), Biomechanics second editon, p143-144, Springer-Verlag.

Skalak R., et al. (1973), “Strain energy function of red blood cell membranes,” Biophys. J. 13, 245-264.